Terahertz electromagnetic radiation from intrinsic Josephson junctions at zero magnetic field via breather-type self-oscillations

V. M. Krasnov

Department of Physics, AlbaNova University Center, Stockholm University, SE-10691 Stockholm, Sweden

(Received 18 April 2011; revised manuscript received 20 April 2011; published 27 May 2011)

I propose a new mechanism of intense high-frequency electromagnetic wave generation by spatially uniform stacked Josephson junctions at zero magnetic field. The ac-Josephson effect converts the dc-bias voltage into ac supercurrent; however, in the absence of spatial variation of the Josephson phase difference it does not provide dc-to-ac power conversion, needed for emission of electromagnetic waves. Here I demonstrate that at geometrical resonance conditions, spatial homogeneity of the phase can be spontaneously broken by the appearance of breathers (bound fluxon-antifluxon pairs), facilitating effective dc-to-ac power conversion. This leads to self-oscillations at cavity-mode frequencies, accompanied by the emission of radiation. The proposed mechanism explains all major features of recently observed THz radiation from large-area $Bi_2Sr_2CaCu_2O_{8+x}$ mesa structures.

DOI: 10.1103/PhysRevB.83.174517 PACS number(s): 74.72.Gh, 74.50.+r, 74.78.Fk, 85.25.Cp

I. INTRODUCTION

Self-oscillations are self-sustaining oscillations in nonlinear systems with a frequency and often an amplitude independent of the driving force. Oscillatory behavior in plasma,[1] the operation of a clock, multivibrators, voice, and the sound of musical instruments all are examples of self-oscillations. Typically, periodic self-oscillations are excited by a constant force. The frequency is determined either by an internal resonance (e.g., a cavity mode) or a characteristic relaxation time. Self-oscillations are widely used for the generation of microwaves, for example, in magnetrons, klystrons, and Gunn diodes.[2]

Recently, a significant THz emission has been reported at zero magnetic field from large-area $Bi_2Sr_2CaCu_2O_{8+x}$ (Bi-2212) mesa structures,[3–5] which represent natural stacks of atomic-scale intrinsic Josephson junctions (IJJs). Although the emission occurs at geometrical resonance frequencies,[5] association with conventional Fiske steps[6] is problematic because their amplitude is zero at $H = 0$. Furthermore, significant emission power would require a large quality factor $Q \gg 1$ (Ref. 7). Since the Q of Fiske steps is inversely proportional to the mesa size,[6] it is not clear how it could be sufficiently large for large mesas with high operation temperatures due to self-heating. Therefore, the observed radiation is quite puzzling and remains a matter of intense discussion.[5,7–14]

Here I propose a new mechanism of emission from spatially *uniform* stacked Josephson junctions at $H = 0$ via spontaneous breather-type self-oscillations. Breathers are bound fluxon-antifluxon pairs with zero net flux.[15] They effectively couple ac-Josephson oscillations to the dc-bias, which allows resonant excitation of cavity modes and leads to significant THz emission. It is argued that breather-type self-oscillations explain all experimental features of zero-field emission from large Bi-2212 mesas.

Radiation from large IJJs is following the ac-Josephson relation.[3–5] Although the ac-Josephson effect converts the dc-bias voltage into the oscillating supercurrent, this does not ensure emission because the supercurrent is nondissipative and cannot by itself pump energy from the dc-power supply into radiation. Such a dc-to-ac *power* conversion can be achieved via the Lorentz force,

$$F_L = sI \times B \tag{1}$$

(per junction), where I is the dc-bias current and s is the stacking periodicity ($s \simeq 1.5$ nm for IJJs). Emission by means of the ac-Josephson effect requires *finite* $B_i(x) \neq 0$, which is connected with the finite Josephson phase gradients $\nabla\varphi_i \neq 0$ (i is the junction index). The main unanswered question is how $B \neq 0$ appears at $H = 0$.

The paper is organized as follows. In Sec. II, different Josephson and non-Josephson mechanisms of emission from stacked IJJs are briefly reviewed. In Sec. III, the theoretical formalism, used in numerical simulations, is described. To study the radiation emission from the stack, we employ the coupled sine-Gordon equation[16] with dynamic radiative boundary conditions.[7] In Sec. IV, the main results are presented and discussed. We also discuss the role of the quality factor and the limiting, detrimental effect of self-heating and estimate the emission power from Bi-2212 mesas. Finally, we analyze the consistency of the proposed mechanism with experimentally observed zero-field emission from large Bi-2212 mesa structures. The supplemental material[17] provides instructions to the free demo program, which can be used for direct analysis of various dynamic states in stacked Josephson junctions.

II. MECHANISMS OF EMISSION FROM STACKED JOSEPHSON JUNCTIONS

As emphasized in the Introduction, the presence of the ac-Josephson effect is not sufficient for achieving radiation emission from Josephson junctions. dc-to-ac power conversion is essential. Below I briefly review known Josephson and non-Josephson emission mechanisms at zero magnetic field.

A. Inhomogeneity and self-field effects

Structural inhomogeneity may lead to some coupling of the dc bias to the ac-resonance field at $H = 0$ (Refs. 9 and 18). The inhomogeneity can be caused by variation of the critical current

density, nonuniform bias current distribution, or a thermal gradient.[19] In large Bi-2212 mesas the inhomogeneity can also be induced by uneven self-heating at large bias[11] and by defects in Bi-2212 single crystals. Associated phase gradients lead to distortion of the Fraunhofer pattern $I_c(H)$,[19] which can be attributed to a self-field caused by the nonuniform current flow. This may lead to the appearance of zero-field Fiske steps.[18] However, they can hardly explain the observed emission from Bi-2212: Large flux quantization field in atomic scale IJJs would require a too large inhomogeneity.[9] Furthermore, such inhomogeneity could hinder mutual synchronization of IJJs (Ref. 6) and suppress collective Fiske resonances, required for coherent amplification of the emission power.

B. Trapped vortices

Fluxons create a large phase gradient $\simeq\pi/\lambda_J$ (λ_J is the Josephson penetration depth) and an effective dc-to-ac-power conversion. Usually, fluxons are introduced by applying an in-plane magnetic field. In long Josephson junctions, $L \gg \lambda_J$, they can be trapped at $H = 0$. Emission scenarios, involving quasistatic semifluxons/antifluxons[8] or fluxons/antifluxons[10] in mesas were proposed. For a single junction static fluxon-antifluxon pairs are unstable, because they tend to annihilate. However, for stacked junctions fluxon-antifluxon pairs in neighbor junctions are stable.[20,21] Metastable fluxon-antifluxon modes at $H = 0$ were clearly observed in large Bi-2212 mesas, as they cause multiple valued critical current.[20] Fluxons experience the Lorentz force, which facilitates efficient pumping of the dc power into the fluxon energy. Upon collision and annihilation of fluxons at junction edges, radiation pulses are produced. Significant flux-flow emission from stacked junctions requires both stabilization of the square (in-phase) fluxon lattice and high-quality geometrical resonances.[7] For IJJs, this can only be achieved at strong fields, $H > \Phi_0/\lambda_J s \simeq 2T$, and for small mesas.[6,22] None of those requirements is realized in case of zero-field emission from large mesas.

C. Electrostriction

The presence of ionic dielectric polarization in BiO layers of Bi-2212 leads to generation of c-axis phonons or phonon polaritons at the ac-Josephson frequency. Recently, it has been demonstrated that very-high-power densities $\sim$kW/cm^2 can be achieved in small mesas.[23] Such emission may occur at zero field, but phonons, rather than photons, are emitted.

D. Non-Josephson mechanisms: Zero-field steps, Cherenkov radiation, and nonequilibrium emission

Several non-Josephson emission mechanisms at $H = 0$ are also known. Stable fluxon-antifluxon pairs in stacked junctions can be unbound by a transport current and may start shuttling in the stack, leading to appearance of zero-field steps (ZFS) in I–V curves.[21] Some emission does take place at ZFS;[24,25] however, it occurs at subharmonics of the Josephson frequency[24] and the emission power is small because the fluxon is not annihilated, but is reflected as an antifluxon upon collision with the edge.

In stacks, ZFS can be accompanied by non-Josephson Cherenkov radiation due to partial decomposition of fluxons into traveling plasma waves.[26–28]

Also, recombination of injected nonequilibrium quasiparticles leads to generation of bosons.[13,29] The nonequilibrium emission is direct (does not involve the ac-Josephson effect) and can provide very high efficacy.[13] It is most effective at $H = 0$ because it benefits from the sharp gap singularity in the quasiparticle density of states.

III. NUMERICAL FORMALISM

Analysis of emission from stacked Josephson junctions requires the implementation of proper nonlocal radiative boundary conditions[7] into the coupled sine-Gordon equation. The emission is facilitated by the finite radiation impedance Z. Simulations are made at $H = 0$ for $N = 10$ identical, uniform junctions with parameters typical for optimally doped Bi-2212 IJJs.[6,22] A variety of dynamic states for different stack parameters can be explicitly seen using a provided demo program.[17] Instructions to the program are given in the supplemental material.

IJJs exhibit hysteresis, that is, remain underdamped, almost up to T_c (Ref. 30). To take into account temperature variation, the damping parameter was varied from strongly underdamped $\alpha = 0.01$ (low T) to overdamped $\alpha = 1$ (high T). The emission power scales with the width of the stack w and is normalized to $w = 20\ \mu$m.

A. The coupled sine-Gordon equation

We consider a stack with the overlap geometry, consisting of $N = 10$ junctions with the following parameters: J_{ci}, the critical current density; C_i and R_i, the capacitance and the quasiparticle resistance per unit area, respectively; t_i, the thickness of the tunnel barrier between the layers; d_i and λ_{Si}, the thickness and London penetration depth of superconducting layers, respectively; and L, the lengths of the stack along the x axis. The elements of the stack are numerated from the bottom to the top, so that junction i consists of superconducting layers i, $i + 1$ and the tunnel barrier i.

The gauge invariant phase differences, φ_i, in the stack can be described by the coupled sine-Gordon equation[16]:

$$\varphi'' = \mathbf{A} \cdot \mathbf{J}_z - \mathbf{J}_b. \tag{2}$$

Here φ is the column of φ_i, "primes" denote spatial derivatives (in x axis), $\mathbf{A}$ is a symmetric tridiagonal $N \times N$ matrix with nonzero elements $A_{i,i-1} = -S_i/\Lambda_l$; $A_{i,i} = \Lambda_i/\Lambda_l$; $A_{i,i+1} = -S_{i+1}/\Lambda_l$. Here $\Lambda_i = t_i + \lambda_{Si}\coth(\frac{d_i}{\lambda_{Si}}) + \lambda_{Si+1}\coth(\frac{d_{i+1}}{\lambda_{Si+1}})$, $S_i = \lambda_{Si}\mathrm{cosech}(\frac{d_i}{\lambda_{Si}})$. Parameters in the equations above are normalized to those in the junction $i = l$.

$\mathbf{J}_z$ is the vector representing the current density across the junctions, which consists of three main components, the supercurrent, the displacement current, and the normal (quasiparticle) current:

$$J_{zi} = j_{ci}\sin(\varphi_i) + \tilde{C}_i\ddot{\varphi}_i + \alpha_i\dot{\varphi}_i. \tag{3}$$

Here $j_{ci} = \frac{J_{ci}}{J_{cl}}$, $\tilde{C}_i = \frac{C_i}{C_l}$, "dots" denote time derivatives and $\alpha_i = \sqrt{\frac{\Phi_0}{2\pi c J_{ci} C_l R_i^2}}$ is the damping parameter, Φ_0 is the flux quantum, and c is the velocity of light in vacuum.

In Eq. (3), $\mathbf{J}_b$ represents the bias current density.[27,28] In Eqs. (2) and (3) space and time are normalized to the Josephson penetration depth, $\lambda_{Jl} = \sqrt{\frac{\Phi_0 c}{8\pi^2 J_{cl} \Lambda_l}}$, and the inverse plasma frequency $1/\omega_{pl} = \sqrt{\frac{\Phi_0 C_l}{2\pi c J_{cl}}}$ of a single junction l, respectively.

For a stack of N Josephson junctions, phase velocities of transverse electromagnetic waves, propagating along the junctions, are split into N modes with velocities[31]

$$c_n = c_0 \left[1 - 2S\cos\left(\frac{\pi n}{N+1}\right)\right]^{-1/2}, \; n = 1,2,\ldots,N, \quad (4)$$

where $c_0 = c\sqrt{t_l/\varepsilon_r \Lambda_l}$ is Swihart velocity of a single JJ (#l) and ε_r is the dielectric constant of the barrier. The slowest velocity c_N corresponds to out-of-phase mode with opposite direction of the electric field in neighbor junctions. The fastest c_1 corresponds to the in-phase mode with similar direction of field in all the junctions in the stack.

Calculations are presented for a stack with $N = 10$ identical junctions with parameters typical for optimally doped Bi-2212: $d = 6$ Å; $t = 9.5$ Å; the stacking periodicity of IJJs $s = d + t = 15.5$Å; J_c=1050 A/cm^2; λ_s=1244 Å, which corresponds to the effective London penetration depth $\lambda_{ab} = \lambda_s\sqrt{s/d} = 200$ nm; the dielectric constant was $\varepsilon_r \simeq 8.5$, corresponding to the Swihart velocity $c_0 = 4.42 \times 10^5$ m/s and the slowest out-of-phase mode velocity $c_N = 3.16 \times 10^5$ m/s; the Josephson penetration length is $\lambda_J \simeq 0.7$ μm; and Josephson plasma frequency $\omega_p = 6.36 \times 10^{11}$rad/s.

B. Nonlocal radiative boundary conditions

In order to calculate emission from the junctions, dynamic radiative boundary conditions to the sine-Gordon equation must be employed[7]:

$$\frac{\partial\varphi}{\partial x}(x = 0,L) = \left(H \pm \mu_0 \frac{E_{ac}(0,L)}{Z}\right) \frac{2\pi\lambda_{Jl}\Lambda_l^*}{\Phi_0}. \quad (5)$$

Here H is the applied in-plane magnetic field in the y-axis direction and $\Lambda_l^* = \Lambda_l - S_l - S_{l+1}$ is the effective magnetic thickness of the junction #l. E_{ac} is the dynamic (instantaneous) value of the ac component of the electric field outside the junctions and Z is the effective radiative impedance, which facilitates emission from the junctions (emission is zero for $Z = \infty$). Plus and minus signs correspond to the left $x = 0$ and right $x = L$ edges of the junction, respectively, because the direction of emission is opposite at opposite edges. In stacked junctions E_{ac} is nonlocal and is the result of interference of electric fields from all junctions:

$$E_{ac} = \sum_{i=1}^{N} E_i. \quad (6)$$

Radiative losses are associated with additional currents flowing through edges of the stack:

$$\Delta I_{rad} = wE_{ac}/Z. \quad (7)$$

Those displacementlike currents should be added to the bias term at the edges of the junctions.

The net emission power from one edge of the stack is

$$P_{rad} = wt_0 H_{ac} \sum_{i=1}^{N} E_i = wt_0 E_{ac}^2/Z. \quad (8)$$

Equations (5)–(7) together form the final nonlocal dynamic boundary conditions for stacked Josephson junctions. For the out-of-phase state, $E_i = -E_{i+1}$, $E_{ac} = 0$, they reduce to the nonradiative Neumann-type boundary condition. For the in-phase state, $E_i = E_{i+1}$, $E_{ac} = NE_i$, they lead to coherent power amplification $\propto N^2$ [Eq. (8)].

C. Effect of temperature and self-heating

Self-heating of Bi-2212 mesas[32] leads to reduction of the quality factor of geometrical resonances and ultimately limits the efficiency of emission. $Q \propto 1/\alpha$ depends strongly on T and decreases rapidly with increasing temperature. In the present model the damping parameter and Q are assumed to be constant, independent of N and bias. That is, self-heating at large bias is not explicitly taken into account. In this oversimplified case the collective in-phase mode is equally stable no matter how many junctions are there in the stack. This has been checked in simulations for different N, which showed that the absolute value of electric and magnetic fields and the modulation of phase are almost independent of N for a given set of other parameters, because they depend only on Q. In this case the proportionality of $P_{rad} \propto N^2$ is achieved automatically (per definition). The only N dependence appears in resonance voltages, due to continuing growth of the in-phase velocity $c_1(N)$ for $N < 400$ (Ref. 6).

To describe the experimental situation, the strong detrimental effect of self-heating on Q as a function of N and bias voltage must be taken into account. Assuming that the main effect of self-heating is the increase of damping $\alpha(T)$, qualitatively the influence of self-heating can be obtained from comparison of simulations for the same stack with different damping parameters presented in Figs. 1–3: Larger damping corresponds to higher T.

More details on the description of the coupled sine-Gordon formalism, geometrical resonances, and radiative boundary conditions in stacked Josephson junctions can be found in Refs. 27 and 28, 6 and 7, respectively. A recent overview of self-heating can be found in Ref. 33.

IV. RESULTS AND DISCUSSION

Figure 1(a) shows I–V characteristics for stacks with the length $L = 20\lambda_J$ and $\alpha = 0.01$. Different colors represent simulations with different initial conditions, corresponding to different amount of trapped fluxons and antifluxons. At low bias this leads to the appearance of ZFS (Ref. 21). At larger bias, distinct resonances appear, resembling Fiske steps. Resonant modes (m,n) in a stack are described by the wave numbers $k_{ab} = m\pi/L$ in plane and $k_c = n\pi/Ns$ in the c-axis direction.[31]

Figure 1(b) shows a normalized radiation power P_{rad} (from one edge). All presented simulations are made for very large radiation impedance Z, so that radiative losses

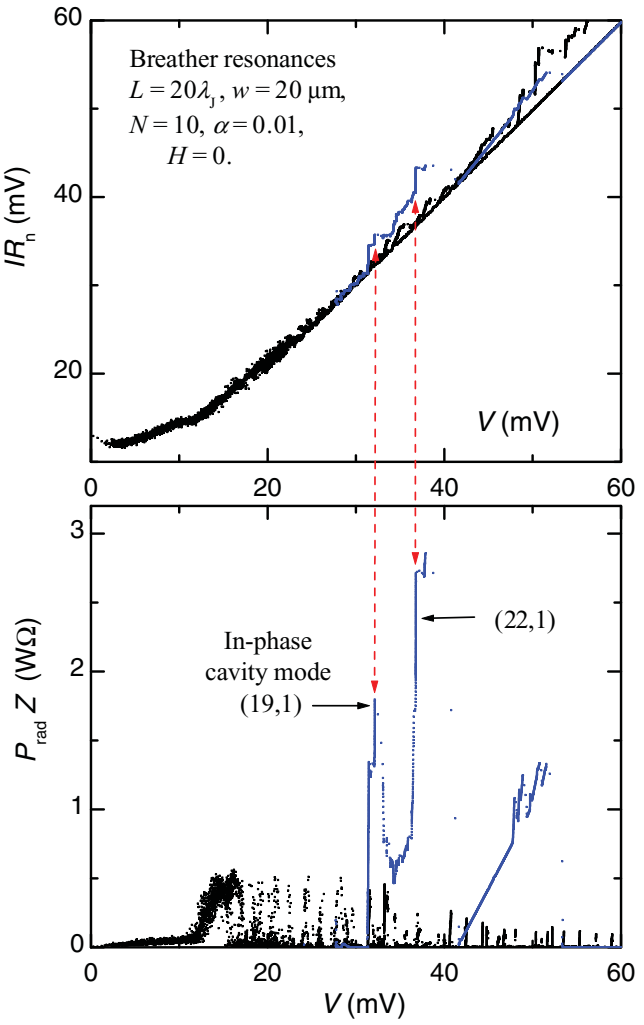

FIG. 1. (Color online) (a) Normalized I–V characteristics for uniform, underdamped stack Josephson junctions at zero applied field. Pronounced steps, caused by breather self-oscillations, are seen. Different colors correspond to simulations with different amounts of trapped fluxons/antifluxons at $I = 0$. It is seen that breather resonances are metastable and depend on initial conditions. (b) Normalized radiative power along the same I–V's. Pronounced maxima occur at collective in-phase cavity resonances, indicated by arrows.

are much smaller than internal resistive losses. Under those circumstances, the product $P_{\rm rad} Z$ is independent of Z (Ref. 7). From Figs. 1(a) and 1(b) it is seen that only certain steps are accompanied by strong emission, while others are not, just like in the case of Fiske steps.[6,7] In Fig. 1(b) it is indicated that distinct emission maxima occur at collective in-phase cavity modes (19,1) and (22,1) due to coherent amplification of radiation from the stack.[7]

Figure 2 shows snapshots of spatial distributions of phases φ_i, magnetic inductions B_i ($\simeq$0.18 G per division), and ac components of voltages V_i ($\simeq$0.2 mV per division) for different resonances: (a) for overdamped $\alpha = 1$ and (b)–(d) underdamped $\alpha = 0.1$ stacks with $L = 20\lambda_J$. The junction color code is shown in Fig. 2(a). Clear two-dimensional standing wave patterns are seen, typical for cavity modes in the stack.[6,7,31]

From Fig. 2 it is seen that there is no increment of phase in the junctions $\varphi_i(x = 0) = \varphi_i(L)$, which means that the net magnetic flux in each junction is zero. The observed modulation of phase is, therefore, caused by a spontaneous formation of ordered breather lattice, consisting of similar breather chains in each junction. Breather chains couple to the dc-power supply via the Lorentz force and effectively pump energy into ac-Josephson oscillations. This makes breather resonances self-sustaining, once ignited. The frequency of oscillations is adopted to the nearest cavity mode in the stack. Such behavior is typical for self-oscillation phenomena, as mentioned in the Introduction.

The breather amplitude is not quantized and the phase variation can acquire any value in the range $-2\pi < \Delta\varphi_i < 2\pi$. Figure 2(a) shows a special case, when the maximum $\Delta\varphi_i$ is close to $\pm\pi$, similar to the case discussed in Ref. 8. Figure 2(d) represents the case when breathers have large amplitudes. At some moments fluxons and antifluxons are well separated so that $\Delta\varphi_i \simeq \pm 2\pi$, similar to the case considered in Ref. 10. This state can also be viewed as if there are coexisting fluxon and antifluxon sublattices moving in opposite directions. However, even in those cases, $\Delta\varphi_i$ are not constant but are oscillating in time. In general, the amplitude $\Delta\varphi_i$ can be arbitrary, as shown in Figs. 2(b) and 2(c).

A. Radiation spectrum

Figure 3 shows the spectra of voltage in the middle junction $i = 5$ at the edge of the stack $x = 0$. Frequency is normalized by the Josephson plasma frequency ω_p. Results are shown for overdamped stacks $\alpha = 1$ with $L = 20\lambda_J$ (solid line) and $L = 100\lambda_J$ (dashed line), biased at the same relative current $I/I_c = 1.4$ and having the same dc voltage. For $L = 20\lambda_J$ it corresponds to the in-phase resonance (2,1), shown in Fig. 2(a), and for $L = 100\lambda_J$ to the in-phase mode (10,1), with the same spatial separation between nodes. It is seen that radiation spectra are similar and consist of sharp maxima at the primary Josephson frequency ω_J and several harmonics, similar to experimental observations.[5]

B. Quality factor of breather resonance

Simulations in Fig. 3 demonstrate that self-oscillations are not hampered even in overdamped and very long stacks. Furthermore, neither the amplitude nor the linewidth of oscillations is deteriorated in the longer stack. This implies that the Q's of both resonances are similar. Quality factors of geometrical resonances were considered in Ref. 6: For the mode (m,n), $Q_{m,n} = m\pi(c_n/c_0)(\lambda/L)/\alpha$, where c_n is the velocity of mode n and c_0 is the Swihart velocity of a single junction. Using the approximate (valid for $N < 400$) expression for c_1 (Ref. 6), we obtain for the most important in-phase mode $n = 1$:

$$Q_{m,1} \simeq \frac{m\sqrt{2}(N+1)}{(L/\lambda_J)\alpha}. \qquad (9)$$

It is seen that modes with the same L/m from Fig. 3 indeed have the same $Q \simeq \sqrt{2} > 1$, despite junctions that are long and overdamped. The quality factor of the junction, $Q_0 = 1/\alpha$,

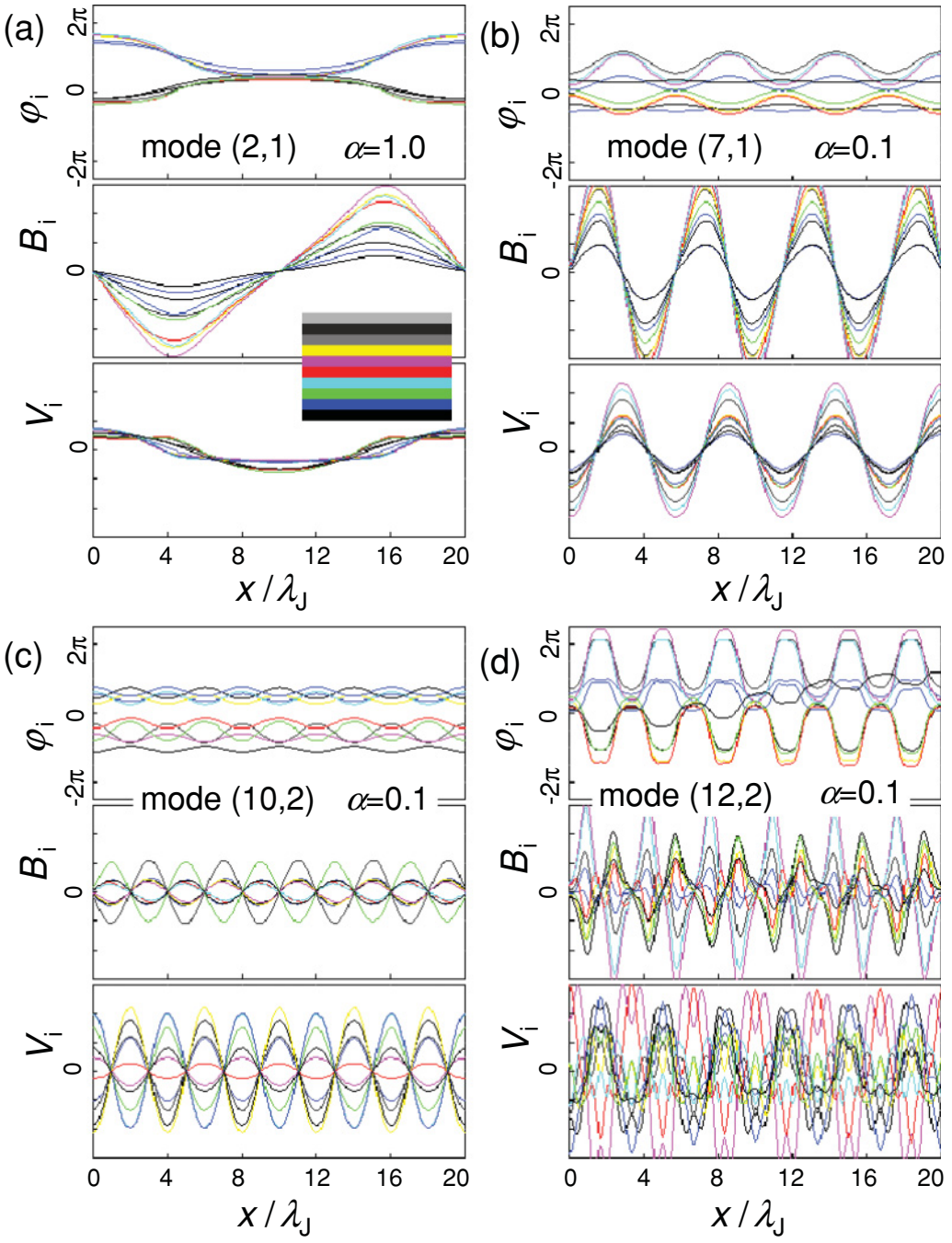

FIG. 2. (Color online) Snapshots of phases φ_i, magnetic inductions B_i, and ac component of voltages V_i at four different breather resonances for $L = 20\lambda_J$ overdamped $\alpha = 1$ (a) and underdamped $\alpha = 0.1$ (b)–(d) stacks. It is seen that electromagnetic field forms standing-wave patterns in the stack. Excited cavity modes (m,n) are indicated in the figures. Panels (a) and (b) represent coherently emitting modes $n = 1$ with in-phase oscillations in all junctions. Panels (c) and (d) show nonemitting $n = 2$ modes with one half of the stack out of phase with the other.

should not be confused with that for geometrical resonances $Q_{m,n} = (\omega_{m,n}/\omega_p)Q_0$.

I want to address the question raised in Ref. 12: why the resonant state is established, provided it has much larger energy than the nonresonant (McCumber) state. Apparently, the resonance with large $\Delta\varphi_i$, B_i, and V_i correspond to a sharp maximum in the junction energy. However, it effectively pumps out the energy stored in the dc-power supply (the battery). Therefore, the total energy of the system, the junctions plus the battery, is rapidly decreasing.

C. Emission power

Let us estimate the emission power from Bi-2212 mesas. At the in-phase geometrical resonance $P_{\rm rad} \propto N^2Q^2$ (Ref. 7). Here N^2 and Q^2 terms represent the coherent and the resonant amplification factors, respectively. The latter is rapidly decreasing with increasing temperature. Due to self-heating, mesas with large N at large bias become overdamped. The ac-voltage amplitude in this case can be obtained from the corresponding simulation in Fig. 2(a): $V_i \simeq 0.1$ mV. The

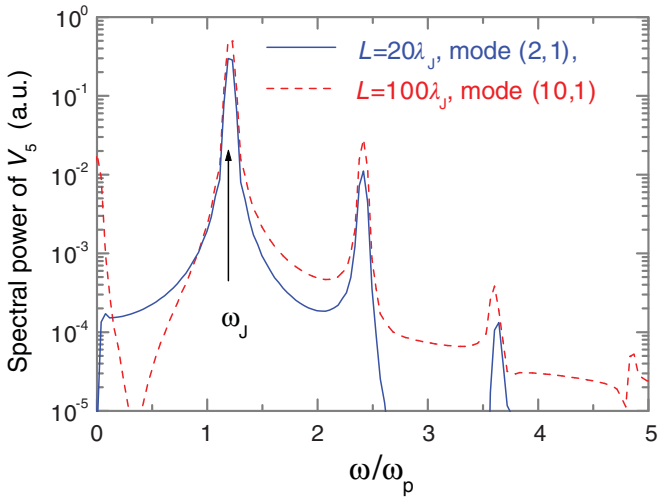

FIG. 3. (Color online) Spectra of voltage oscillations in the middle junction for overdamped stacks, $\alpha = 1$, with $L = 20\lambda_J$ and $100\lambda_J$ at $H = 0$. Stacks are biased at $I = 1.4I_c$ and have the same dc voltage, corresponding to in-phase cavity modes (2,1) and (10,1), respectively. Spectra are similar and have narrow maxima at the Josephson frequency ω_J. Note that amplitudes and linewidths of the two resonances are similar, despite different L.

emission power in the in-phase state is $P_{\rm rad} = (NV_i)^2/R_{\rm rad}$, where $R_{\rm rad}$ is the effective radiative resistance.[7] Assuming it is of the order of the free-space impedance $R_{\rm rad} \sim 100\Omega$, we obtain for the stack with $N = 100$ IJJs, $P \sim 1\ \mu$W, consistent with the reported values.[3] The power in this case is limited by small Q (Ref. 7), which in turn is limited by self-heating, rather than the size of the mesa or N.

V. CONCLUSIONS

In conclusion, a new mechanism of zero-field radiation from stacked Josephson junctions is proposed, via spontaneous breather-type self-oscillations at geometrical resonance conditions. It explains all major experimental features of THz emission from large Bi-2212 mesas.[3–5]

(i) Breather self-oscillations can lead to powerful coherent radiation from *uniform* mesas at $H = 0$ because breather can effectively couple ac-Josephson oscillations to dc-power supply via the Lorentz force.

(ii) Self-oscillations follow the ac-Josephson relation and occur via resonant excitation of cavity modes.

(iii) Unlike Fiske resonances, the in-phase state is much more robust for breather resonances because of much weaker breather-breather than fluxon-fluxon interaction. In-phase Fiske resonances in the flux-flow state require stabilization of the rectangular fluxon lattice,[22] which is usually unstable due to fluxon-fluxon repulsion.

(iv) Unlike Fiske resonances, which have only one strong mode for a given field (the velocity matching mode with two nodes per fluxon),[6] the wavelength of the breather chain can be arbitrary. This flexibility provides an important advantage with respect to Fiske resonances, because it allows effective excitation of any cavity mode, including unusual ones (e.g., TM modes[5]).

(v) The flexibility of breather resonances ensures that some high-enough in-phase resonance would have large-enough Q, irrespective of damping and junctions length. This allows intense emission with narrow linewidth even in very large mesas and at elevated temperatures.

(vi) Nonuniformity is detrimental (rather than beneficial[9]) in this scenario because it hinders mutual synchronization of junction,[7] needed for coherent emission.

(vii) Small in-plane magnetic field tends to suppress the emission. With increasing field, breather resonances are gradually substituted by Fiske resonances, which have smaller amplitude at low fields.

(viii) Breather resonances depend on the initial conditions. This leads to metastability of emission, observed in Bi-2212 mesas.[3] Essentially, self-oscillations must be ignited to become self-sustainable. Here they were ignited with the help of trapped fluxons/antifluxons. The ignition can also be facilitated by nonequilibrium current injection,[13,29] which is most intense just beneath bias electrodes, consistent with observation in Ref. 4.

(ix) The coherent emission power $P_{\rm rad} \propto N^2Q^2$ is initially increasing as N^2 with increasing N, but eventually slows down because of progressive self-heating, which reduces Q of the cavity mode. From Eq. (2) it follows that Q is enhanced up to $N \simeq 400$, which is probably the optimal number of IJJs for achieving a large coherent amplification N^2 without too large degradation of Q as a result of self-heating. Self-heating ultimately limits the emission efficiency from large Bi-2212 mesas.

Finally, I note that spontaneous breaking of spatial uniformity at $H = 0$ via breather formation has been observed in discrete Josephson junction arrays.[34] It was shown that such breathers can excite geometrical resonances in junctions.[35] I also want to note some similarity between the emitting breather-type self-oscillations in stacked Josephson junction, discussed here, with emitting dipole-type self-oscillations in semiconducting superlattices.[2] Indeed the dipole, consisting of charge accumulation and depletion layers (domains), can be viewed as an analog of the breather.

ACKNOWLEDGMENTS

Financial support from the Swedish Research Council the SU-Core Facility in Nanotechnology and the K & A Wallenberg Foundation is gratefully acknowledged.

[1] S. K. Zhdanov, M. Schwabe, R. Heidemann, R. Sütterlin, H. M. Thomas, M. Rubin-Zuzic, H. Rothermel, T. Hagl, A. V. Ivlev, G. E. Morfill, V. I. Molotkov, A. M. Lipaev, O. F. Petrov, V. E. Fortov, and T. Reiter, New J. Phys. **12**, 043006 (2010).

[2] L. L. Bonilla and H. T. Grahn, Rep. Prog. Phys. **68**, 577 (2005).

[3] L. Ozyuzer, A. E. Koshelev, C. Kurter, N. Gopalsami, Q. Li, M. Tachiki, K. Kadowaki, T. Yamamoto, H. Minami, H. Yamaguchi,

T. Tachiki, K. E. Gray, W.-K. Kwok, and U. Welp, Science **318**, 1291 (2007).
[4]H. B. Wang, S. Guenon, B. Gross, J. Yuan, Z. G. Jiang, Y. Y. Zhong, M. Grüenzweig, A. Iishi, P. H. Wu, T. Hatano, D. Koelle, and R. Kleiner, Phys. Rev. Lett. **105**, 057002 (2010).
[5]M. Tsujimoto, K. Yamaki, K. Deguchi, T. Yamamoto, T. Kashiwagi, H. Minami, M. Tachiki, K. Kadowaki, and R. A. Klemm, Phys. Rev. Lett. **105**, 037005 (2010).
[6]S. O. Katterwe, A. Rydh, H. Motzkau, A. B. Kulakov, and V. M. Krasnov, Phys. Rev. B **82**, 024517 (2010).
[7]V. M. Krasnov, Phys. Rev. B **82**, 134524 (2010).
[8]X. Hu and S. Z. Lin, Supercond. Sci. Technol. **23**, 053001 (2010).
[9]A. E. Koshelev and L. N. Bulaevskii, Phys. Rev. B **77**, 014530 (2008).
[10]A. E. Koshelev, Phys. Rev. B **78**, 174509 (2008).
[11]H. B. Wang, S. Guenon, J. Yuan, A. Iishi, S. Arisawa, T. Hatano, T. Yamashita, D. Koelle, and R. Kleiner, Phys. Rev. Lett. **102**, 017006 (2009).
[12]M. Tachiki, S. Fukuya, and T. Koyama, Phys. Rev. Lett. **102**, 127002 (2009).
[13]V. M. Krasnov, Phys. Rev. Lett. **103**, 227002 (2009); **97**, 257003 (2006).
[14]T. Tachiki and T. Uchida, J. Appl. Phys. **107**, 103920 (2010).
[15]D. W. McLaughlin and A. C. Scott, Phys. Rev. A **18**, 1652 (1978).
[16]S. Sakai, P. Bodin, and N. Pedersen, J. Appl. Phys. **73**, 2411 (1993).
[17]See supplemental material at [http://link.aps.org/supplemental/10.1103/PhysRevB.83.174517] for access to a demo program, showing a variety of dynamic states in stacked junctions.
[18]C. Camerlingo, M. Russo, and R. Vaglio, J. Appl. Phys. **53**, 7609 (1982).
[19]V. M. Krasnov, V. A. Oboznov, and N. F. Pedersen, Phys. Rev. B **55**, 14486 (1997).
[20]V. M. Krasnov, V. A. Oboznov, V. V. Ryazanov, N. Mros, A. Yurgens, and D. Winkler, Phys. Rev. B **61**, 766 (2000).
[21]R. Kleiner, T. Gaber, and G. Hechtfischer, Phys. Rev. B **62**, 4086 (2000).
[22]S. O. Katterwe and V. M. Krasnov, Phys. Rev. B **80**, 020502(R) (2009).
[23]S. O. Katterwe, H. Motzkau, A. Rydh, and V. M. Krasnov, Phys. Rev. B **83**, 100510(R) (2011).
[24]B. Dueholm, O. A. Levring, J. Mygind, N. F. Pedersen, O. H. Soerensen, and M. Cirillo, Phys. Rev. Lett. **46**, 1299 (1981).
[25]J. J. Chang, J. T. Chen, M. R. Scheuermann, and D. J. Scalapino, Phys. Rev. B **31**, 1658 (1985).
[26]G. Hechtfischer, R. Kleiner, A. V. Ustinov, and P. Müller, Phys. Rev. Lett. **79**, 1365 (1997).
[27]V. M. Krasnov and D. Winkler, Phys. Rev. B **56**, 9106 (1997).
[28]V. M. Krasnov, Phys. Rev. B **63**, 064519 (2001).
[29]I. Iguchi, K. Lee, E. Kume, T. Ishibashi, and K. Sato, Phys. Rev. B **61**, 689 (2000).
[30]V. M. Krasnov, T. Golod, T. Bauch, and P. Delsing, Phys. Rev. B **76**, 224517 (2007).
[31]R. Kleiner, Phys. Rev. B **50**, 6919 (1994).
[32]V. M. Krasnov, M. Sandberg, and I. Zogaj, Phys. Rev. Lett. **94**, 077003 (2005).
[33]V. M. Krasnov, Phys. Rev. B **79**, 214510 (2009).
[34]E. Trias, J. J. Mazo, and T. P. Orlando, Phys. Rev. Lett. **84**, 741 (2000); P. Binder, D. Abraimov, A. V. Ustinov, S. Flach, and Y. Zolotaryuk, *ibid.* **84**, 745 (2000).
[35]I. Ottaviani, M. Cirillo, M. Lucci, V. Merlo, M. Salvato, M. G. Castellano, G. Torrioli, F. Mueller, and T. Weimann, Phys. Rev. B **80**, 174518 (2009).